Strength of Materials, Vol. 38, No. 6, 2006

FATIGUE STRENGTH OF AN ($\alpha + \beta$)-TYPE TITANIUM ALLOY Ti–6Al–4V PRODUCED BY THE ELECTRON-BEAM PHYSICAL VAPOR DEPOSITION METHOD

O. N. Gerasimchuk,[a] G. A. Sergienko,[b] V. I. Bondarchuk,[b] A. V. Terukov,[b] Yu. S. Nalimov,[a] and B. A. Gryaznov[a]

UDC 539.4;669.295

The fatigue test results are presented for an ($\alpha + \beta$)-type titanium alloy Ti–6Al–4V in the form of two-layered smooth specimens (the first layer is a condensate prepared by the electron-beam physical vapor deposition method, the second one is a substrate from a standard sheet material of the same type) and condensate specimens. It has been found that the presence in the condensate of deposition defects such as droplets lowers the fatigue limit of the material by approximately 1.5 times as compared to that of the condensate which is free of defects. It is shown that in the absence of droplets, the fatigue limit of the condensate is no lower than that of the substrate material. The microstructure, texture and fracture surfaces of the materials under study are analyzed, on the basis of which the fatigue limits of the defectless condensate and substrate material are calculated using approaches of linear fracture mechanics. Good agreement has been obtained between calculated and experimental data.

Keywords: fatigue limit, physical vapor deposition method, titanium alloy, condensate, droplets, microstructure, texture.

Introduction. The electron-beam physical vapor deposition (EB PVD) method refers to up-to-date means of producing a great variety of materials [1]. As compared to conventional techniques, it offers a number of advantages enabling creation of materials with unique characteristics. Thus, using this method it is possible to produce layered and gradient (i.e., with variable chemical composition and microstructure) coatings, materials with controlled porosity, alloys with chemical composition that cannot be obtained using the majority of conventional techniques, and also materials with a special controllable structure [1, 2]. All this gives grounds for introduction of this technique into the production of materials for the state-of-the-art technology, application of coatings on finished products in order to improve their characteristics.

At the same time, some limitations are inherent in the EB PVD method as, in essence, in any other technique. From the standpoint of structure of the material produced by this method, the most widespread defects are droplets. They occur as a result of the temperature gradient in the direction of the normal to the liquid bath surface and are solidified microdroplets which, after leaving the melt surface, have reached the substrate [1]. Microdroplets, which are foreign inclusions with structure (and, on frequent occasions, chemical composition) that differ from the surrounding material, serve as stress raisers adversely affecting the mechanical properties of the EB PVD condensate.

Titanium alloys are important structural materials widely used in modern engineering. However, by now, there exists a limited number of studies devoted to the problem of producing these alloys by the EB PVD method [3, 4]. The mechanical properties of titanium and its alloys deposited by the above method, the effect of structure and defects upon them have been investigated still less. The goal of the present work was to determine the fatigue strength characteristics of the Ti–6Al–4V alloy deposited by the EB PVD method and to elucidate the effect of structural defects (microdroplets), which are peculiar to this technique, on its behavior under cyclic loading.

[a]Pisarenko Institute of Problems of Strength, National Academy of Sciences of Ukraine, Kiev, Ukraine. [b]Kurdyumov Institute of Physics of Metals, National Academy of Sciences of Ukraine, Kiev, Ukraine. Translated from Problemy Prochnosti, No. 6, pp. 113 – 121, November – December, 2006. Original article submitted May 23, 2005.

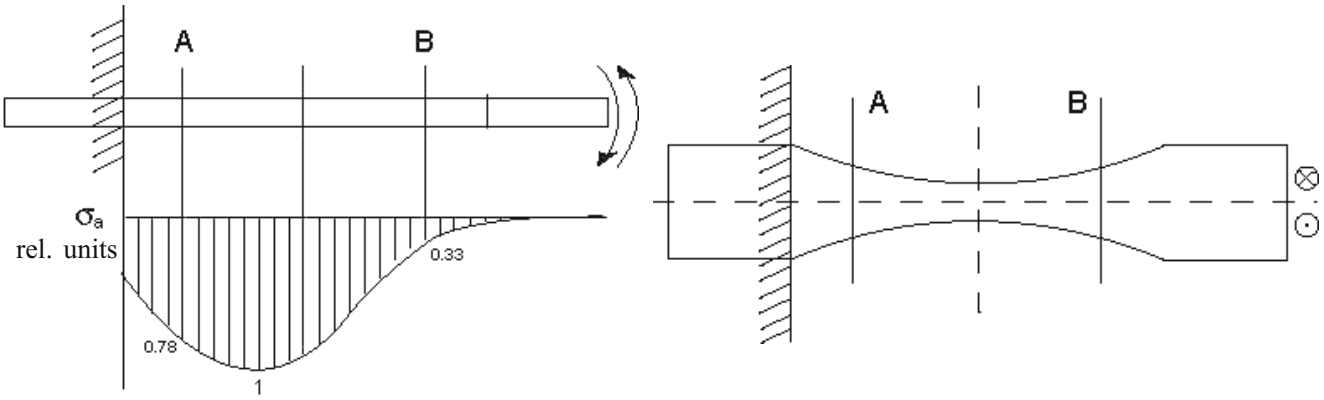

Fig. 1. Loading scheme, stress distribution diagram, and specimen shape for fatigue testing (points *A* and *B* indicate the range of failure areas along the specimen length).

Materials and Investigation Procedures. Using the EB PVD method, a titanium alloy coating was obtained by deposition on plane substrates of the Ti–6Al–4V alloy. Prior to evaporation, the substrate surface was polished. A rod of a similar alloy made by the TIMET corporation was used as a material to be evaporated.

The alloy microstructure was studied using the optical microscopy; the crystallographic structure was studied by the x-ray method using a DRON-3 type unit with a special-purpose goniometer developed at the Kurdyumov Institute of Physics of Metals, National Academy of Sciences of Ukraine. Fractographic studies were carried out using a "CamScan" scanning electron microscope.

The fatigue strength characteristics were studied experimentally according to the procedure described in detail in [5]. Flat cantilever specimens with a working cross section of 1 mm in thickness and 5 mm in width were tested in lateral bending using a VÉDS-400A type electrodynamic vibrator under resonant transverse vibration condition. The criterion of the specimen failure was the drop in the frequency by 1% as compared to the initial resonance value, which corresponded to the occurrence of a 0.5 mm deep surface macrocrack in the working section of the specimen under testing. The specimen shape and stress distribution diagram experimentally determined as a function of bending are presented in Fig. 1. Prior to testing, specimen surfaces were polished, sharp edges were rounded off ($r \approx 0.5$ mm) to eliminate stress raisers. Three types of specimens were cycled: 1) specimens prepared from the condensate; 2) specimens of the substrate material (conventional sheet of Ti–6Al–4V); and 3) the so-called composite specimens prepared from the substrate material with a 300 to 700 μm condensate layer deposited onto one side. Noteworthy is that, in the process of the strain gage calibration of specimens, no differences between the moduli of elasticity of the substrate and condensate were observed.

Results and Their Discussion. The microstructure of the composite specimens prepared by the EB PVD method is shown in Fig. 2. It is evident that the microstructures of the condensate and substrate differ considerably. A bimodal microstructure formed as a result of the previous thermomechanical treatment is characteristic of the substrate. The microstructure contains primary α-phase grains of sizes approximately 10×20 μm, somewhat elongated in the direction of rolling, which are separated by areas of the β-phase wherein plates of the secondary α-phase are observed. The condensate consists of needle-shaped α-grains (of 3–4 μm in diameter and 10–15 μm along the long axis) elongated in the direction of growth interlayered with areas of the β-phase between them. At the very beginning of the evaporation, a droplet was deposited on the substrate, as a result of which the condensation surface swelled above it forming a raised portion on the external surface of the condensate. Two peculiar features are seen: a through "column" of more coarse grains as compared to the bulk condensate that was grown on the microdroplet, and the porosity around this column near its origin induced by the effect of the "leader of growth" of microdroplets [1]. The formation of coarse grains behind the microdroplet is likely to be induced by the elevated temperature of condensation on the surface raised portion. (In what follows, we will take the name "droplets" instead of "microdroplets with accompanying columns"). Light bands on the micrographs correspond to the condensate layers enriched by aluminum.

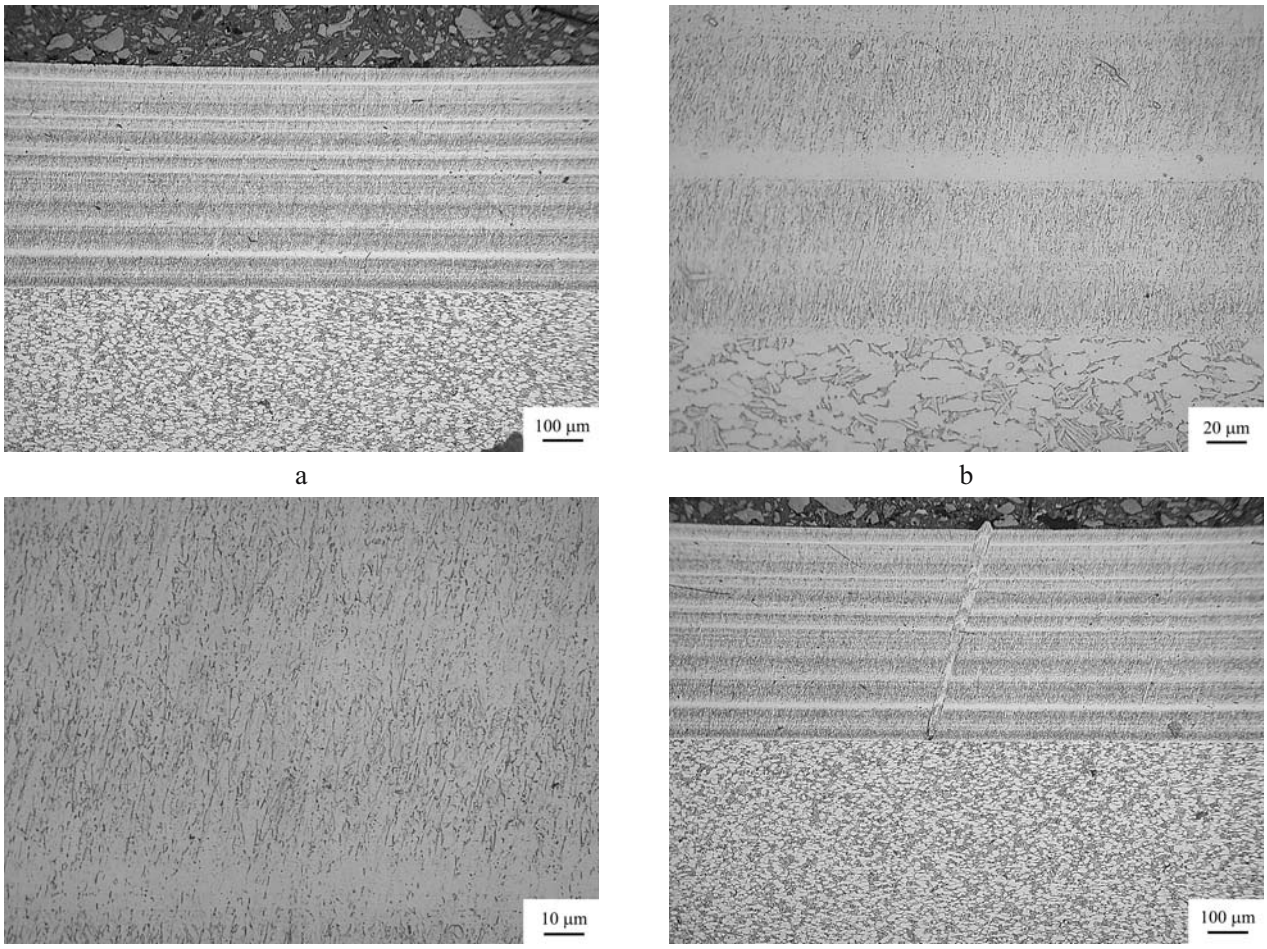

Fig. 2. Microstructure of the composite specimens prepared by the EB PVD method: (a) a general view (the substrate is below, the condensate is above); (b) the substrate-condensate boundary; (c) the condensate microstructure; (d) the microdroplet in the condensate deposited at the very beginning of the process of evaporation (the through column grown on the microdroplet and the raised portion on the external surface are seen).

The high-cycle fatigue limit σ_{-1} was determined for 10^7 cycles. In order to obtain additional data, the specimens unfailed during the prescribed number of cycles were retested at higher loads. The fatigue test results for 30 composite specimens are given in Fig. 3. The specimens unfailed at 10^7 cycles are presented by two values of the stress amplitude: the maximum stress amplitude and stress at the fracture site during retesting (see Fig. 1). It is seen that the experimental points can be divided into two groups approximated by the curves with their corresponding fatigue limits of about 500 and 300 MPa.

To clarify the causes for this scatter and determine the microstructural factors responsible for the formation of cracks of critical sizes in the specimens, fractographic studies were carried out. It was found that in the specimens of the second group, a critical crack was nucleated in the condensate, at the place where relatively large droplets appear on the specimen surface (Fig. 4). At the same time, almost all specimens of the first group failed on the side of the substrate, and no traces of droplets were observed on the surfaces of fracture (Fig. 5). The data of the fractographic investigations make it possible to suggest that in the specimens of this group, a critical crack was nucleated in large particles of the primary α-phase that appear on the surface.

To analyze more fully the influence of the defects such as droplets on the fatigue strength characteristics of the alloy under investigation, specimens of the condensate with a high content of droplets, standard Ti–6Al–4V (the substrate) and composite material with a low content of droplets in the condensate were tested (Fig. 6). As shown by

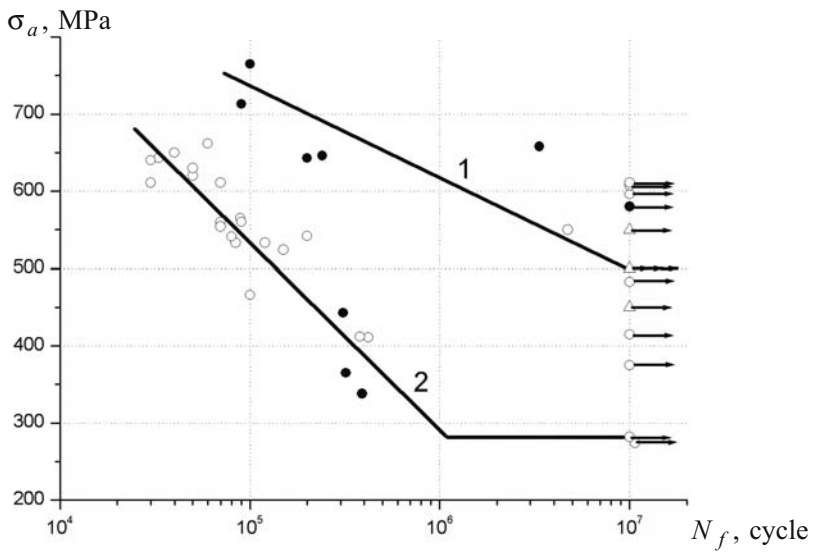

Fig. 3. Fatigue test results for composite specimens: (*1*) large droplets were absent in the working sections of the specimens; (*2*) the fracture has started from large droplets in the cross section [(○) is for the stress at the fracture site; (●) is for the stress at the fracture site during retesting; (△) is for the maximum value of the stress amplitude].

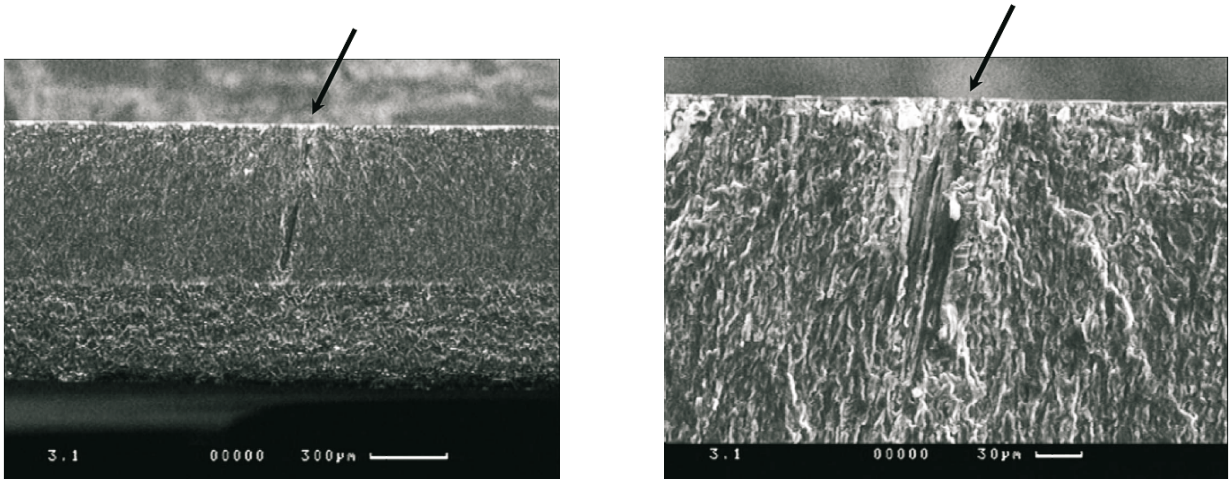

Fig. 4. Fracture surface of the composite specimen (curve *2* in Fig. 3). The condensate is above, substrate is below, and the arrows indicate the point of nucleation of the critical crack (the droplet appearance on the condensate surface).

fractographic studies, in all specimens of the condensate, the critical cracks were nucleated at the point where a large droplet appears on the surface (Fig. 7). The fatigue limit of the condensate is close to 300 MPa, which is in good agreement with the above results obtained for the composite specimens containing droplets. At the same time, the fatigue limit of the composite specimens containing a limited number of droplets as that of the substrate material, is close to 500 MPa, which also agrees with the results obtained for the composite specimens without large droplets in the working section.

Fractographic analysis testifies to the absence of the correlation between the geometrical parameters of the droplet (diameter, depth) and fatigue characteristics. Essentially all droplets had different dimensions and shape (see, for example, Figs. 4 and 7). This problem requires further, deeper study of the effect of defects such as droplets on the fatigue strength characteristics.

The results obtained are also analyzed from the standpoint of linear fracture mechanics using the approaches described earlier [6, 7].

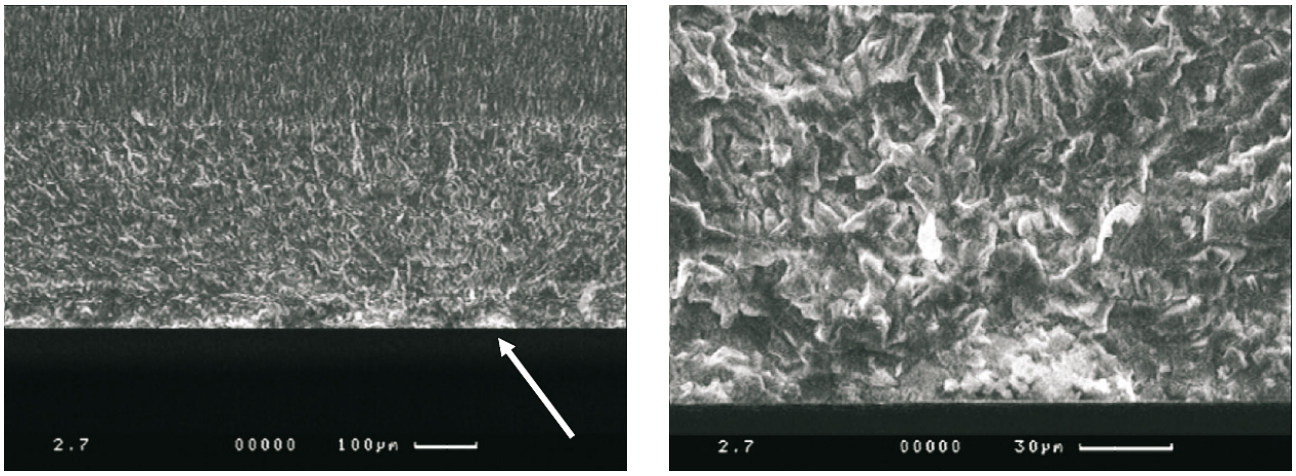

Fig. 5. Fracture surface of the composite specimen (curve *1* in Fig. 3). The condensate is above, substrate is below, and the arrow indicates the point of nucleation of the critical crack (the substrate).

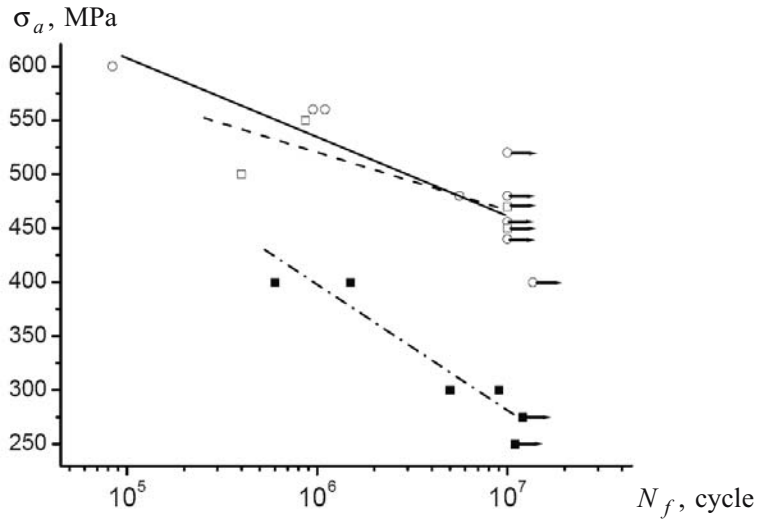

Fig. 6. Fatigue test results for the condensate (■), standard Ti–6Al–4V (□) and composite (○) materials.

The fatigue limits of the defectless condensate and substrate materials were calculated from the relationship

$$\sigma_{-1} = \frac{\Delta K_{th\,eff}}{Y\sqrt{d}},$$

where σ_{-1} is the fatigue limit in bending, $\Delta K_{th\,eff}$ is the effective range of the threshold stress intensity factor, which can be approximately defined as $\Delta K_{th\,eff} = BE$, B is the proportionality coefficient, $B \approx 1.6 \cdot 10^{-5}$ m$^{-1/2}$, E is the modulus of elasticity (it is equal to $1.25 \cdot 10^{-5}$ MPa for alloy Ti–6Al–4V), Y is the function that takes into account the geometrical dimensions of the crack and specimen as well as the loading conditions ($Y \approx 1.99$), and d is the size of the structural parameter (mean size of the structural element responsible for the cyclic strength of the given material). The calculation results are presented in the Table 1 in comparison with experimental data.

The calculated values of the fatigue limit agree well with the experimental ones for the defectless condensate and give an underestimation, even though satisfactory, for the substrate material. This discrepancy can be explained as follows. For calculation, the structural parameter size was assumed to be equal to a mean size of the short axis of the α-phase particles. It was noted above that fatigue cracks were nucleated precisely in the α-phase particles (Fig. 5).

TABLE 1. Comparison of the Fatigue Limits of Alloy Ti–6Al–4V Determined Experimentally and Calculated According to the Above Formula

Material	d, μm	σ_{-1}^{exp}, MPa	σ_{-1}^{calc}, MPa	Δ, %
Defectless condensate	3–4	600–500	580–502	~ 2
Substrate	10	500	318	36

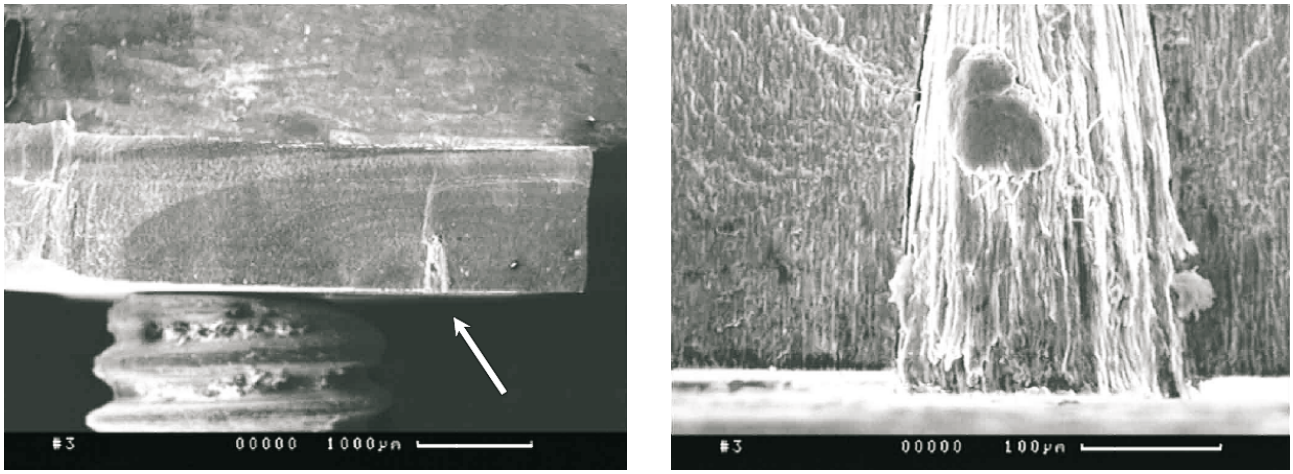

Fig. 7. Fracture surface of the condensate specimen [the condensation direction is top-down; the arrow indicates the site of nucleation of the critical crack (the droplet)].

This is likely to be due to comparatively high stress amplitudes at which specimens were tested. The data are known which testify to the dependence of the mechanism of fatigue fracture of (α + β)-type titanium alloys with a bimodal microstructure on the stress level [8]. At sufficiently high stresses (in this case, specimens which failed on the side of the substrate were tested), an intense gliding of dislocations proceeds in large grains of the α-phase and microcracks are formed. At lower stresses (near the fatigue limit), the difference between the chemical composition of the primary and secondary α-phase is important. As is known, plates separated out during the β-phase are aluminum-depleted as compared to those of the primary α-phase [9]. Therefore, the strength of the primary α-phase is somewhat higher, and at low stresses, the gliding of dislocations is suppressed therein, being proceeded primarily in the colonies of plates of the secondary α-phase (these were more dispersed than particles of the primary α-phase, Fig. 2) where microcracks are nucleated at the level of stresses close to the fatigue limit.

Contrary to the substrate material, the condensate structure contains the α-phase particles of about the same size. Therefore, when calculating σ_{-1} from average size of particles, more accurate agreement is obtained with the experimental value of the fatigue limit for the defectless condensate.

The results obtained have shown that the cyclic strength of the condensate, despite the lower content of aluminum (~ 5 5 mass %), in the absence of defects such as droplets, is not worse than that of the substrate material, which is caused by two factors. Firstly, the condensate microstructure is much more dispersed (Fig. 2) and secondly, the effect of crystallographic texture takes place. As a rule, vapor deposited metals and alloys are characterized by a strong texture [10]. Figure 8 illustrates central areas of pole figures for a basis plane of the α-phase of both the standard material Ti–6Al–4V and condensate. The sheet material of Ti–6Al–4V has a typical texture of deformation in the (α + β)-phase diagram region: the basis planes are mainly oriented at angles of 30–45° to the plane of deformation. The texture of the deposited material is different: the overwhelming majority of crystallites are oriented in a such way that the basis plane is perpendicular to the direction of condensation. Some displacement of the texture axis from the center of the pole figure is caused by that the specimen is cut out from the lateral part of the condensate, i.e., the direction of growth makes a slight angle with the normal to the substrate. As is known, the value of the α-titanium yield strength essentially depends upon its preferred orientation: if the angle between the tensile stress and

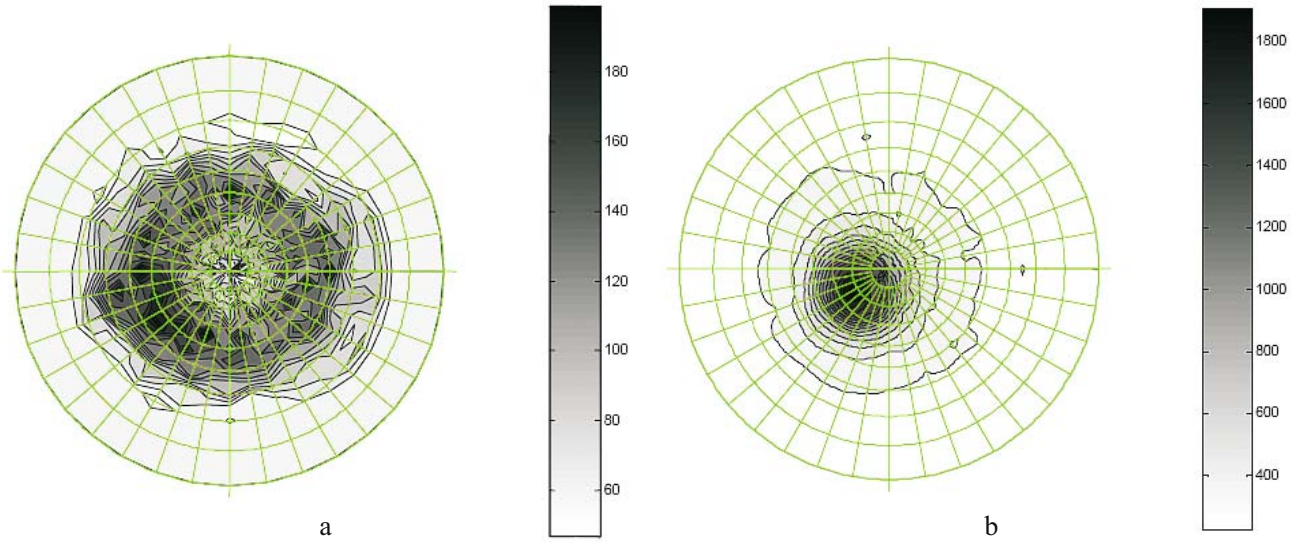

Fig. 8. Pole figures $(0002)_\alpha$ for the standard material Ti–6Al–4V (a) and condensate (b): the plane of the specimens for mechanical testing is parallel to the figure plane (a, b), the condensation direction is perpendicular to the figure plane (b).

crystallographic axis is equal to zero, the value is maximal, whereas at an angle of 45°, it decreases gradually to the minimum, and with increasing angle to 90° it increases again [9]. For the variable loading conditions used, the condensate crystallites are predominantly located at an angle of 90°, whereas the majority of the substrate grains are located at an angle close to 45°. In many cases, the high-cycle fatigue limit of metals and alloys is proportional to the yield strength. Therefore, a very sharp texture of condensation can also result in the increase of the fatigue limit of the defectless condensate as compared to the standard material Ti–6Al–4V, thus compensating the deficiency of aluminum in the condensate.

CONCLUSIONS

1. Defects such as droplets or dropletlike defects are effective stress raisers, and thus adversely affect the fatigue characteristics of the Ti–6Al–4V alloy condensate lowering the fatigue limit by approximately 1.5 times as compared to that of the defectless material.

2. In the absence of droplets, the condensate fatigue limit is no lower than that of the standard sheet alloy Ti–6Al–4V.

3. No correlation between geometrical dimensions of droplets and the fatigue strength characteristics of the condensate is revealed.

4. The fact that defectless Ti–6Al–4V condensate cyclic strength is higher than that of the standard sheet alloy of a similar chemical composition is explained by the microstructure dispersion and presence of the deposition texture in the former material in contrast to the latter.

5. Calculations of the fatigue limit of the materials under study performed from the standpoint of linear fracture mechanics have shown satisfactory agreement with the experimental results.

REFERENCES

1. Z. Schiller, U. Heizieg, and Z. Panzer, *Electron Beam Technology* [in Russian], Énergia, Moscow (1980).
2. B. A. Movchan, “Inorganic materials vapor deposited in vacuum,” in: *Modern Materials Science of the XXI Century* [in Russian], Naukova Dumka, Kiev (1998), pp. 318–332.

3. R. F. Bunshah and R. S. Juntz, “EB PVD of commercially pure titanium,” *Met. Trans*., **4**, No. 1, 21–28 (1973).
4. H. R. Smith, K. Kennedy, and F. S. Boericke, “Metallurgical characteristics of titanium-alloy foil prepared by electron beam evaporation,” *J. Vac. Sci. Technol.*, **7**, No. 6, 48–51 (1970).
5. V. T. Troshchenko, B. A. Gryaznov, Yu. S. Nalimov, et al., “Fatigue strength and cyclic crack resistance of titanium alloy VT3-1 in different structural states. Part 1. Study procedure and experimental results,” *Strength Mater*., **27**, No. 5-6, 245–251 (1995).
6. V. T. Troshchenko, B. A. Gryaznov, Yu. S. Nalimov, et al., “Fatigue strength and cyclic crack resistance of titanium alloy VT3-1 in different structural states. Part 2. Procedure for considering the effect of structure on fatigue limit,” *Strength Mater*., **27**, No. 5-6, 252–256 (1995).
7. O. M. Ivasishin, K. A. Bondareva, V. I. Bondarchuk, et al., “Fatigue resistance of powder metallurgy Ti–6Al–4V alloy,” *Strength Mater*., **36**, No. 3, 225–230 (2004).
8. J. Albrecht and G. Lütjering, “Microstructure and mechanical properties of titanium alloys,” in: *Titanium’99: Science and Technology*, CRISM “Prometey” (2000), **1**, pp. 363–374.
9. G. Lütjering G. and J. C. Williams, *Titanium*, Springer (2003).
10. B. A. Movchan and I. S. Malashenko, *Heat-Resistant Coatings Produced in Vacuum* [in Russian], Naukova Dumka, Kiev (1983).